



CHEMISTRY & SUSTAINABILITY

CHEM **SUS** CHEM

ENERGY & MATERIALS

Accepted Article

Title: Enhanced Furfural Yields from Xylose Dehydration in the gamma-Valerolactone/Water Solvent System at Elevated Temperatures

Authors: Canan Sener, Ali Hussain Motagamwala, David Martin Alonso, and James Dumesic

This manuscript has been accepted after peer review and appears as an Accepted Article online prior to editing, proofing, and formal publication of the final Version of Record (VoR). This work is currently citable by using the Digital Object Identifier (DOI) given below. The VoR will be published online in Early View as soon as possible and may be different to this Accepted Article as a result of editing. Readers should obtain the VoR from the journal website shown below when it is published to ensure accuracy of information. The authors are responsible for the content of this Accepted Article.

To be cited as: *ChemSusChem* 10.1002/cssc.201800730

Link to VoR: <http://dx.doi.org/10.1002/cssc.201800730>

WILEY-VCH

www.chemsuschem.org

A Journal of



Enhanced Furfural Yields from Xylose Dehydration in the γ -Valerolactone/Water Solvent System at Elevated Temperatures

Canan Sener,^[a,b] Ali Hussain Motagamwala,^[a,b] David Martin Alonso,^[a] and James A. Dumesic^{*,[a,b]}

Abstract: High yields of furfural (>90%) were achieved from xylose dehydration in a sustainable solvent system composed of γ -valerolactone (GVL), a biomass derived solvent, and water. It is identified that high reaction temperatures (e.g., 498 K) are required to achieve high furfural yield. Additionally, it is shown that the furfural yield at these temperatures is independent of the initial xylose concentration, and high furfural yield is obtained for industrially relevant xylose concentrations (10 wt%). A reaction kinetics model is developed to describe the experimental data obtained with solvent system composed of 80 wt% GVL and 20 wt% water across the range of reaction conditions studied (473 – 523 K, 1–10 mM acid catalyst, 66 – 660 mM xylose concentration). The kinetic model demonstrates that furfural loss due to bimolecular condensation of xylose and furfural is minimized at elevated temperature, whereas carbon loss due to xylose degradation increases with increasing temperature. Accordingly, the optimal temperature range for xylose dehydration to furfural in the GVL/H₂O solvent system is identified to be from 480 to 500 K. Under these reaction conditions, furfural yield of 93% is achieved at 97% xylan conversion from lignocellulosic biomass (maple wood).

Introduction

The primary challenge for the sustainable production of fuels and chemical intermediates (e.g. alcohols, aldehydes, acids) from renewable biomass resources is to develop cost-effective processes to transform highly functionalized feedstock into value-added chemicals.^[1–8] In this regard, furfural can be produced by acid-catalyzed dehydration of the pentoses obtained from renewable biomass resources. Furfural has been identified by the US-DOE as one of the top 30 building block chemicals that can be produced from lignocellulosic biomass, and it is considered as a platform molecule which can be upgraded to various platform compounds that are suitable for replacing or supplementing petroleum-derived commodity chemicals, fuels and fuel

additives.^[1,9] Furfural is currently used in refining lubrication oils, as a fungicide, and mostly in the production of resins via the production of furfuryl alcohol, which accounts for more than 75% of the global furfural consumption. Producing furfural more effectively and at lower cost may enable other promising technologies, such as the production of furan through decarbonylation, and in production of tetrahydrofuran (THF) through hydrogenation of furan, providing a biomass-based route for the production of industrial solvents. Furfural may also serve as a building block for potential transportation fuels like 2-methylfuran and 2-methyltetrahydrofuran.^[10–12] As such, furfural can be used to bridge the gap between carbohydrate chemistry and petroleum-based industrial chemistry.^[13] The global furfural solvent market is expected to reach USD 153.4 million by 2022. Industrially, furfural is mainly produced from xylose obtained by acid-catalyzed hydrolysis of biomass rich in pentosan, such as corn cobs, oat hulls and bagasse. Many commercial processes have been developed, including the Quaker Oats process, AGRIFURANE process, and the ROSENLEW process; however, the highest furfural yield achieved in these processes is approximately 50%.^[14] To improve the process, various catalysts and solvent systems have been developed;^[15,16] however, the yields are still limited by the formation of undesired by-products, humins,^[17,18] which are proposed to be produced by condensation of furfural with xylose or an intermediate formed during xylose dehydration to furfural.^[19] Several strategies have been developed to minimize the formation of humins during xylose dehydration to furfural to increase furfural yield. One promising strategy is to use a bi-phasic system wherein furfural produced in the aqueous phase during the reaction is continuously extracted in the organic phase.^[20,21] The organic phase is chosen such that both xylose and the acid catalyst do not partition into the organic phase, and the furfural extracted into the organic phase is protected from condensation as well as catalytic degradation.^[22–24] Accordingly, increased furfural yields of ~60-70% have been reported with the use of biphasic systems; however, most organic solvents have shown poor partitioning of furfural into the organic phase, necessitating large amount of organic solvent for continuous extraction.^[20] Solvents like 2-sec-butylphenol, 4-n-hexylphenol and 2-methoxy-4-propylphenol have been employed for furfural production due to their high partition coefficient for furfural,^[25] but these solvents are toxic and are not ideal for industrial application. Another strategy employed to improve the production of furfural is the addition of salts to form of a bi-phasic system.^[26] For example, NaCl has been utilized to improve the partitioning of furfural to the organic phase while using more environmentally benign organic solvents;^[27,28] however, salt leads to corrosion of the reactor and also creates additional waste stream leading to a non-sustainable process. In addition to the

[a] Dr. C. Sener, A. H. Motagamwala, Dr. D. M. Alonso, Prof. J. A. Dumesic
Department of Chemical and Biological engineering
University of Wisconsin-Madison
Madison, Wisconsin 53706 (USA)
E-mail: jdumesic@wisc.edu

[b] Dr. C. Sener, A. H. Motagamwala, Prof. J. A. Dumesic
DOE Great Lakes Bioenergy Research Center, Wisconsin Energy
Institute
1552 University Ave.
Madison, Wisconsin 53726 (USA)

FULL PAPER

use of organic solvents, ionic liquids have also been used successfully to produce furfural in biphasic as well as monophasic systems.^[29,30] Another alternative to remove furfural from the reaction medium is the use of gas or steam stripping. Yields of 90% have been achieved in these systems, but the high cost of steam or compressed gas is still an impediment for commercial applications.^[31–33] While all of these technologies have demonstrated that it is possible to produce furfural at high yield, they are normally limited to low initial xylose concentration. In addition, the scale up of processes based on the removal of furfural is challenging, as typically mass transfer issues must be addressed. It is thus desirable to have a process which leads to high furfural yield at high initial xylose concentrations and utilizes environmentally friendly solvent systems.

We have recently shown that using a monophasic solvent system composed of a mixture of γ -valerolactone and water is advantageous to produce furfural from xylose^[34,35]. Recently, several novel catalysts have been used with this solvent system to improve furfural yields. Lin et al. used a SO_3H -functionalized ionic liquid as catalyst to produce furfural in GVL at low temperature (413 K) obtaining 78% furfural yield.^[36] Similar yields were obtained by Zhu et al. using a functionalized porous carbon catalyst.^[37] Li et al. employed sulfonated catalysts to achieve up to 93% furfural yield from corn-stover;^[38] however, high catalyst loading (ca. 30 wt%), irreversible deactivation of the sulfonated catalyst and low initial biomass loading (ca. 2wt%) still limit the applicability of this process at commercial scale.

With the goal to maximize the utilization of lignocellulosic biomass, we have shown that the GVL system can be used to efficiently fractionate biomass into three separate streams: a stream containing xylose and furfural, which accounts for >95% of hemicellulose present in the biomass; a high purity cellulose stream, accounting for >90% cellulose present in the initial biomass, and a stream consisting of lignin that retains the functionalities present in the original biomass.^[39] The carbohydrate stream containing the xylose can be dehydrated to produce furfural from the hemicellulose fraction of biomass. In the present work, we have studied and optimized process parameters for dehydration of xylose to furfural, including reaction temperature, acid type, acid concentration, initial xylose concentration, and solvent composition for a monophasic solvent system composed of γ -valerolactone, a biomass derived solvent, and water. We show that under optimal reaction conditions, xylose degradation is minimized leading to high furfural yield. We develop a reaction kinetics model to describe xylose dehydration across a range of experimental conditions. We show that an environmentally benign monophasic solvent system can be used to efficiently dehydrate xylose, at high concentrations, to furfural. Moreover, the reactor set-up presented is simple, as it does not involve phase separations, purification and extractions and eliminates the need for salt and other promoters. Our findings provide directions for reactor design and operational parameter determination for maximizing furfural yields.

Results and Discussion

Temperature Effect

The effect of reaction temperature on dehydration of xylose was studied with 2 wt% (133 mM) xylose over a temperature range from 443 to 523 K and at acid concentrations of 1 mM HCl (open symbols) and 5mM HCl (solid symbols) in a solvent system containing 80 wt% GVL, as shown in Figure 1. The initial rate of xylose consumption and furfural yield increased with increasing temperature, and high furfural yield (>80%) was achieved at 498 K and 523 K with a residence time of 120 seconds and 60 seconds, respectively. The effect of temperature on furfural selectivity is shown in Figure 2.

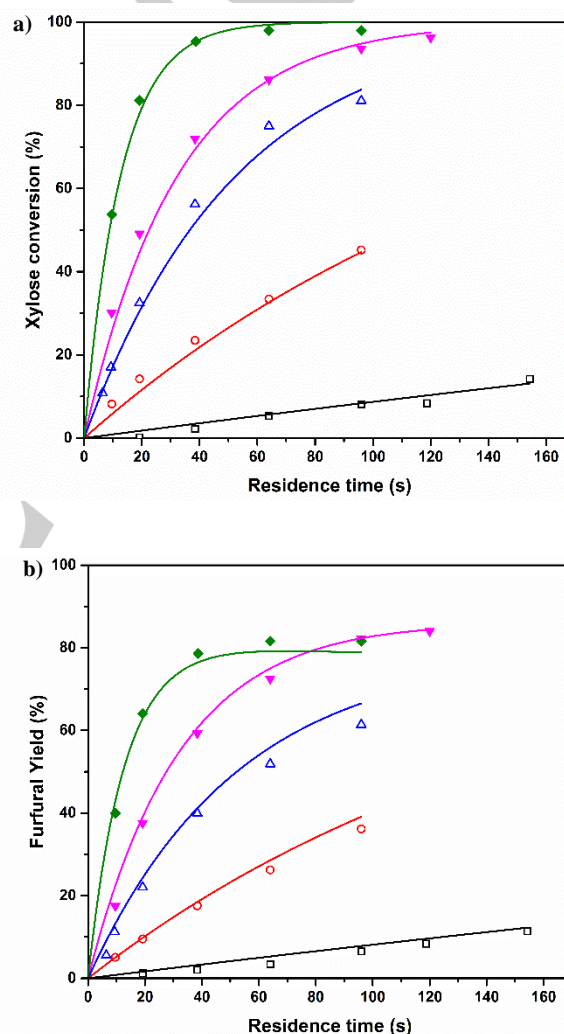


Figure 1. Effect of temperature on (a) xylose conversion and (b) furfural yield. Experiments were conducted with 2 wt% xylose concentration in a solvent system containing 80 wt% GVL. Black open squares represent 1 mM HCl and 473 K; red open circles represent 1 mM HCl and 498 K; blue open triangles represent 1 mM HCl and 523 K; pink closed inverted triangles represent 5 mM HCl and 498 K; green closed diamonds represent 5 mM HCl and 523 K. Solid lines are prediction from kinetic model based on Scheme 1.

FULL PAPER

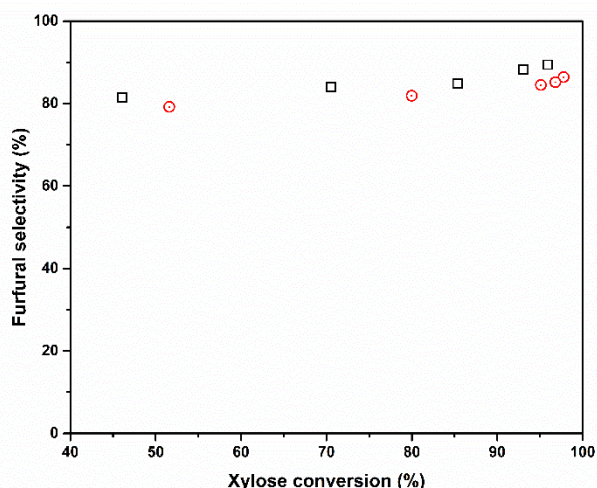


Figure 2. Effect of reaction temperature on furfural selectivity. Experiments were conducted with 2 wt% xylose and 5 mM HCl in a solvent system containing 80 wt% GVL. Black open squares represent 498 K; red open circles represent 523 K.

It is observed that high furfural selectivity is obtained for both reaction temperatures studied. Importantly, it is observed that the selectivity towards furfural remains relatively constant with increasing xylose conversion. This result indicates that minimal furfural degradation occurs due to the condensation of furfural with xylose and/or intermediates produced during xylose dehydration. This behavior is contrary to results obtained in water, where furfural selectivity decreases with increasing xylose conversion.^[19] This fact has important implications for a commercial process where high xylose conversion and high initial xylose concentrations (discussed later) are desired.

Effect of Acid Concentration

The effect of acid concentration on xylose dehydration was studied at acid concentrations of 1, 5 and 10 mM, and at temperatures of 498 and 523 K, as shown in Figure 3. The rate of xylose dehydration increases with increased acid concentration; however, furfural selectivity is independent of acid concentration, as shown in Figure 4. It is observed from Figure 3 that xylose dehydration is first order with respect to the acid concentration, in agreement with previous reports.^[19,35,40] It is observed that the rate of xylose dehydration increases with increasing acid concentration; however, furfural selectivity remains constant at any given xylose conversion (Figure 4). Both the rate and acid concentration have high impact on reactor design, as higher acid concentration leads to higher reaction rate which allows shorter residence time to achieve a given conversion. On the other hand, higher acid concentration leads to faster corrosion and will lower the reactor life. Thus, acid concentration must be judiciously selected to maximize the output from a given reactor setup.

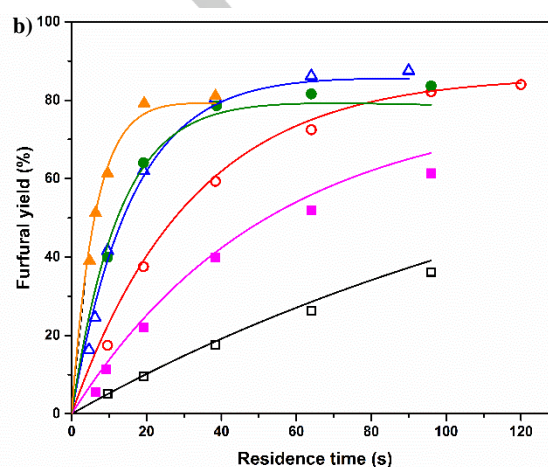
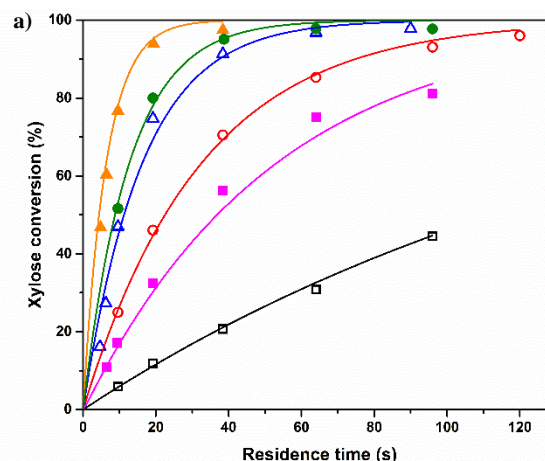


Figure 3. Effect of acid concentration on (a) xylose conversion and (b) furfural yield. Experiments were conducted with 2 wt% xylose concentration in a solvent system containing 80 wt% GVL. Black open squares represent 498 K and 1 mM HCl; red open circles represent 498 K and 5 mM HCl; blue open triangles represent 498 K and 10 mM HCl; pink closed squares represent 523 K and 1 mM HCl; green closed circles represent 523 K and 5 mM HCl; orange closed triangles represent 523 K and 10 mM HCl. Solid lines are prediction from kinetic model based on Scheme 1.

Effect of Xylose Concentration

The effect of xylose concentration on the dehydration of xylose was studied with 5 mM acid concentration at temperatures of 473 and 498 K, as shown in Figure 5. Xylose conversion as well as furfural yield were found to be independent of xylose concentration, indicating that furfural selectivity is independent of the initial xylose concentration, as shown in Figure 6. This behavior is contrary to results obtained in previous studies conducted at lower temperatures, wherein the furfural selectivity decreased with increased xylose (and furfural) concentration.^[35,40]

FULL PAPER

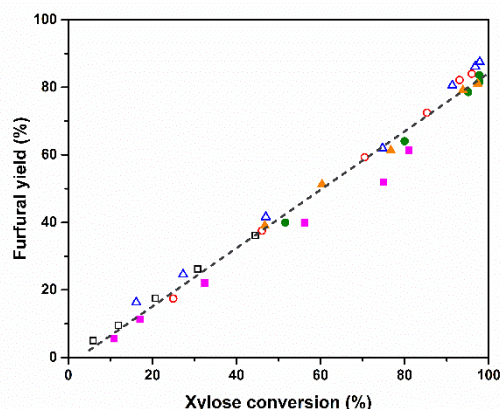


Figure 4. Effect of acid concentration on furfural selectivity. Experiments were conducted with 2 wt% xylose concentration in a solvent system containing 80 wt% GVL. Black open squares represent 498 K and 1 mM HCl; red open circles represent 498 K and 5 mM HCl; blue open triangles represent 498 K and 10 mM HCl; pink closed squares represent 523 K and 1 mM HCl; green closed circles represent 523 K and 5 mM HCl; orange closed triangles represent 523 K and 10 mM HCl. Dashed black line is a visual guide.

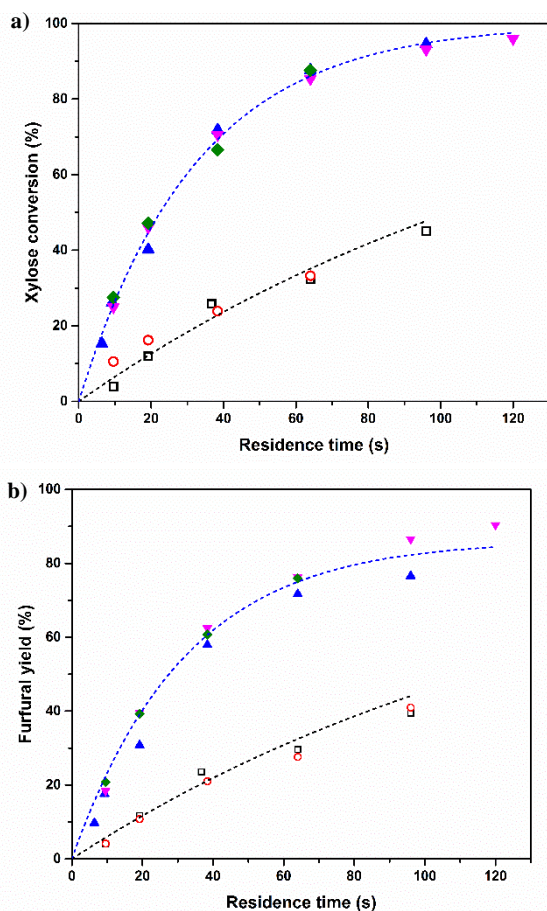


Figure 5. Effect of initial xylose concentration on (a) xylose conversion and (b) furfural yield. Experiments were conducted with 5 mM HCl in a solvent system containing 80 wt% GVL. Black open squares represent 473 K and 1 wt% xylose; red open circles represent 473 K and 4 wt% xylose; blue closed triangles represent 498 K and 1 wt% xylose; pink inverted triangles represent 498 K and 2 wt% xylose; green closed diamonds represent 498 K and 4 wt% xylose. Dashed lines are prediction from kinetic model based on Scheme 1.

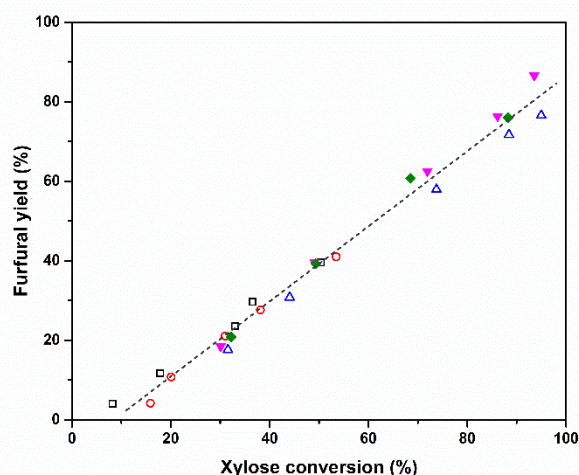


Figure 6. Effect of initial xylose concentration on furfural selectivity. Experiments were conducted with 5 mM HCl in a solvent system containing 80 wt% GVL. Black open squares represent 473 K and 1 wt% xylose; red open circles represent 473 K and 4 wt% xylose; blue closed triangles represent 498 K and 1 wt% xylose; pink inverted triangles represent 498 K and 2 wt% xylose; green closed diamonds represent 498 K and 4 wt% xylose. Dashed black line is a visual guide.

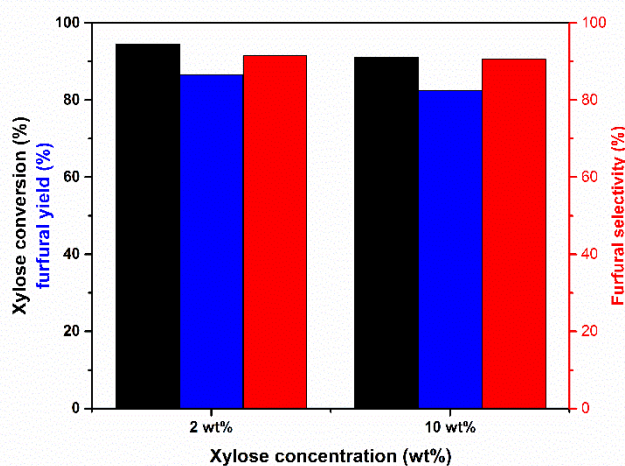


Figure 7. Comparison of furfural yield and selectivity at low and high initial xylose concentrations. Black represents xylose conversion, blue represents furfural yield and red represents furfural selectivity. Experiments were conducted in a solvent system containing 80 wt% GVL at 498 K with 5 mM HCl and a residence time of 96 seconds.

The lower furfural yields in these studies were due to the condensation reaction between xylose and furfural. Therefore, it was suggested to operate dehydration at lower xylose concentration to obtain high furfural selectivity.^[14,19] However, for industrial applications, it is desirable to operate dehydration at high xylose concentrations to reduce separation and overall capital costs. Figure 7 shows a comparison of furfural yield obtained at initial xylose concentrations of 2 and 10 wt% in the

FULL PAPER

GVL/water (80 wt% GVL) solvent system containing 5mM HCl at 498 K. It should be noted that the furfural selectivity is high (>90%), even at high xylose concentration of 10 wt%.

Effect of acid type

Two of the most studied mineral acids for xylose dehydration are hydrochloric acid and sulfuric acid. Accordingly, studies were performed to compare the efficiency of xylose dehydration with these mineral acids, and Figure 8 shows a comparison between the xylose conversion for these two acids. The concentrations of HCl and H₂SO₄ were kept constant at 10 mM even though sulfuric acid is diprotic. This concentration was chosen because the second dissociation constant of sulfuric acid decreases with increasing temperature^[41,42] and sulfuric acid behaves essentially as a mono-protic acid at the temperature used in this study. It can be observed from Figure 8 that the rate of xylose dehydration is higher using hydrochloric acid as the catalyst. However, we observe that the effect of the chloride ion decreases with an increase in temperature (see Figure 8). More importantly, the selectivity to furfural at high xylose conversion is similar for both of these acid catalysts studied, as shown in Figure 9.

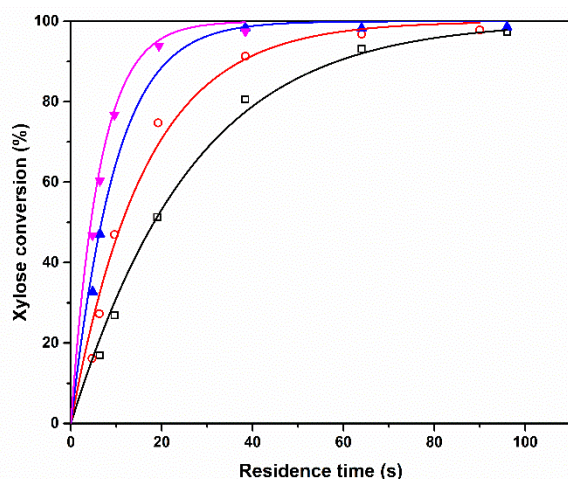


Figure 8. Effect of acid type on xylose dehydration. Experiments were conducted with 2 wt% Xylose in a solvent system containing 80 wt% GVL. Black open squares represent 498 K and 10 mM H₂SO₄; red open circles represent 498 K and 10 mM HCl; blue closed triangles represent 523 K and 10 mM H₂SO₄; pink inverted triangles represent 523 K and 10 mM HCl. Solid lines are visual guides.

It is known that chloride ions promote xylose dehydration reactions,^[43] and the difference observed here between the reactivity of hydrochloric acid and sulfuric acid at 498 K (Figure 8) is an indication of this chloride ion effect. However, the difference in reactivity can also be caused by a difference in dissociation constants of the mineral acids in the GVL/H₂O solvent at elevated temperature. To elucidate the effect of chloride ions on the dehydration of xylose in GVL/H₂O solvent system, NaCl was added to GVL/H₂O solvent containing sulfuric acid, and xylose dehydration was conducted at 443 and 498 K. The results are shown in Figure 10, and it can be observed that the rate of xylose

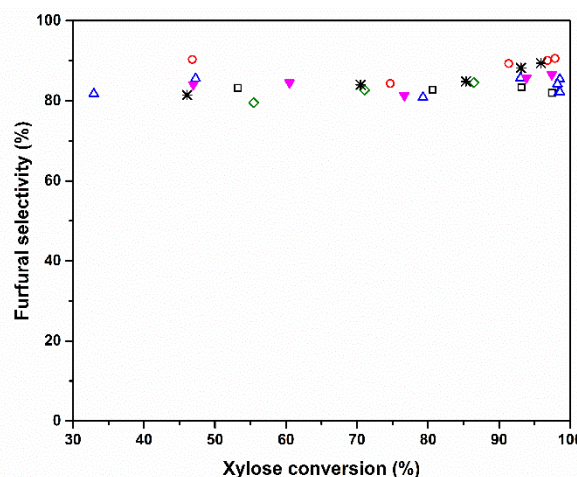
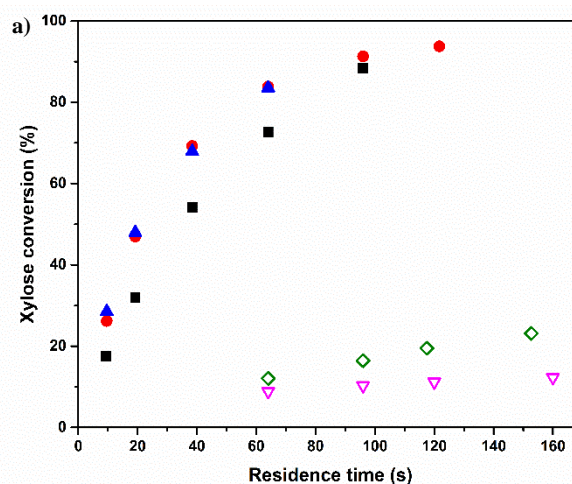


Figure 9. Effect of acid type on Furfural selectivity. Experiments were conducted with 2 wt% Xylose in a solvent system containing 80 wt% GVL. Black open squares represent 498 K and 10 mM H₂SO₄; red open circles represent 498 K and 10 mM HCl; blue open triangles represent 523 K and 10 mM H₂SO₄; pink solid inverted triangles represent 523 K and 10 mM HCl; open green diamonds represent 498 K 5mM H₂SO₄; open black stars represent 498 K and 5mM HCl.

dehydration increases with addition of NaCl, showing the positive effect of the presence of chloride ion on dehydration of xylose. It should be noted that the solvent system is monophasic at these salt concentration (~30 mM) and the improvement observed in furfural yield is not due to the partitioning of furfural to the organic phase. Additionally, it has been shown that the identity of the cation has little effect on the rate of dehydration^[43]. We also show that the effect of chloride ion saturates as the chloride ion concentration increases from 15 to 30 mM (Figure. 10).



FULL PAPER

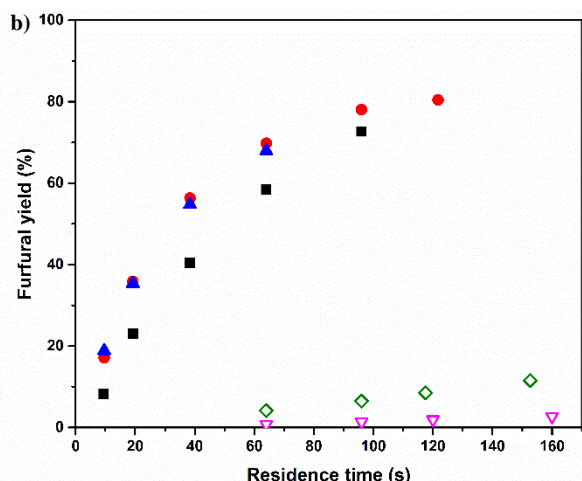


Figure 10. Figure Caption Effect of chloride ion on (a) xylose conversion and (b) on furfural selectivity. Experiments were conducted with 2 wt% Xylose in a solvent system containing 80 wt% GVL. Pink open inverted triangles represent 443 K and 5 mM H₂SO₄; green open diamonds represent 443 K, 5 mM H₂SO₄ and 15 mM NaCl; black solid squares represent 498 K and 5 mM H₂SO₄; red solid circles represent 498 K, 5 mM H₂SO₄ and 15 mM NaCl; blue solid triangles represent 498 K, 5 mM H₂SO₄ and 30 mM NaCl.

Effect of GVL Concentration

We studied the effect of GVL concentration in solvent system on xylose dehydration at temperatures of 498 and 523 K. These studies were performed with solvent systems composed of 70, 80 and 90 wt% GVL. The rate of xylose dehydration increases with increasing GVL concentration, which is in agreement with the literature reports.^[34,35] The furfural yields at high xylose conversion were similar for all studied GVL concentrations (see Figure 11). This behavior is an important advantage when working at high xylose concentrations, as the dehydration of xylose to furfural produces three moles of water for each mole of furfural produced, thereby changing the composition of the solvent as the reaction proceeds.

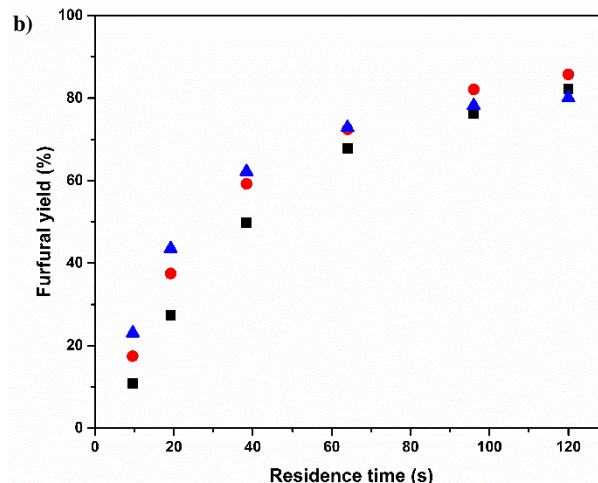
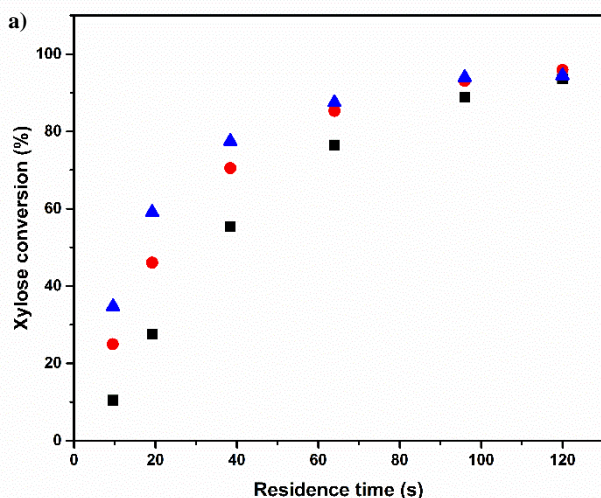


Figure 11. Effect of GVL concentration on (a) xylose conversion and (b) furfural yield. Experiments were conducted with 2 wt% xylose at 498 K with 5 mM HCl. Black squares represent 70 wt% GVL; red circles represent 80 wt% GVL and blue triangles represent 90 wt% GVL.

Reaction Kinetics Analysis

Kinetics of furfural degradation:

We observe high furfural yields under our reaction conditions, indicating that there is minimal furfural degradation. Hence, we first studied the degradation of furfural by self-condensation in the absence of xylose. Figure 12 shows results for furfural degradation at 473, 498 and 523 K with 100 mM HCl and 2 wt% furfural. Note that high acid concentration of 100 mM (20 times of what is required for xylose dehydration) and high residence time were required to achieve appreciable furfural conversion for kinetic analysis. We obtained the rate constant, k_3 , and the activation energy, $E_{a,3}$, for furfural degradation by fitting the data in Figure 12 to the following equation (see Scheme 1, reaction 3)

$$\frac{d[\text{Furfural}]}{dt} = -k_3[\text{Furfural}][\text{H}_3\text{O}^+] \quad [\text{Eq. (1)}]$$

k_3 at the reaction temperature of 498 K, k_3^{498} , was estimated to be $2.85 \times 10^{-2} \text{ M}^{-1}\text{s}^{-1}$ and the activation energy, $E_{a,3}$, was estimated to be $76 \pm 8.4 \text{ kJ/mol}$. These values of k_3^{498} and $E_{a,3}$ were used for modeling furfural degradation throughout this study.

Bimolecular condensation of furfural and xylose:

The high furfural yield obtained in this study indicate that the rate of condensation between xylose and furfural is negligible under our reaction conditions. This behavior is in contrast to the previous reaction kinetics studies of xylose dehydration conducted in GVL/H₂O wherein the loss of xylose and furfural due to condensation reaction was significant.^[35] We also observe that furfural selectivity is independent of initial xylose concentration at the high temperatures of this study (Figure 6 and Figure 7), whereas furfural selectivity would decrease with increasing initial xylose concentration if bimolecular condensation were significant.

FULL PAPER

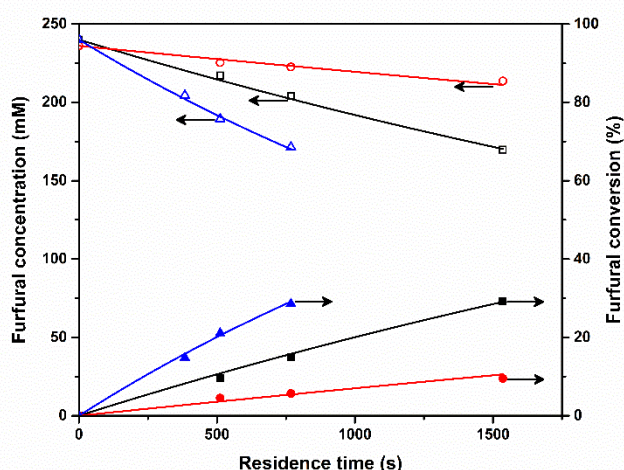


Figure 12. Furfural degradation in presence of 100 mM HCl. Experiments were conducted with 2 wt% Furfural. Furfural concentration is shown with open symbols and furfural conversion is shown with solid symbols. Circles represent experiments conducted at 473 K; squares represent experiments conducted at 498 K, triangles represent experiments conducted at 523 K. Solid lines are predictions from the kinetic model described in equation 3.

It was also shown by Root et al.,^[19] that higher furfural yield of ~60% is obtained in water at high temperature (553 K), whereas low furfural yields (~30-40%) are obtained at lower temperature (453 K). Root et al. proposed that the improved furfural yields at higher temperatures were due to minimal furfural loss by condensation reactions.^[19] Additionally, condensation reactions are analogous to polymerization reactions, and like the polymerization reaction, the condensation reaction becomes insignificant at elevated temperatures.^[44] We also performed experiments to study the conversion of xylose in the presence of furfural in GVL/H₂O using hydrochloric acid as catalyst at 498 K. Figure 13(a) shows the concentration of xylose and furfural as a function of the residence time, and Figure 13(b) shows the xylose conversion and the furfural yield as a function of the residence time. We note here that furfural yield is calculated by subtracting the initial furfural concentration from the furfural concentration obtained after reaction. It can be seen from Figure 13 that high concentrations of initial furfural do not affect xylose dehydration to furfural, indicating that condensation reactions are diminished under the reaction conditions studied. In view of these findings, we can neglect any losses from condensation reactions.

Kinetic study of xylose dehydration:

Reaction kinetics analyses of xylose dehydration to furfural were based on reaction Scheme 1, which includes dehydration of xylose to furfural as a single step, direct xylose degradation, and direct furfural degradation.

Reaction orders with respect to xylose and furfural were found to follow apparent first-order kinetics for all reaction steps in the reaction network. This behavior is in agreement with previous studies showing apparent first-order rates for xylose and furfural in aqueous media using mineral acids as catalyst.^[40,43,45] Also, the rates of xylose and furfural disappearance are proportional to the

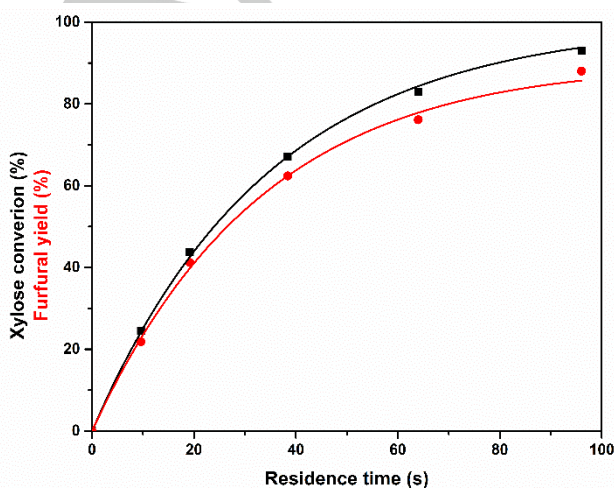
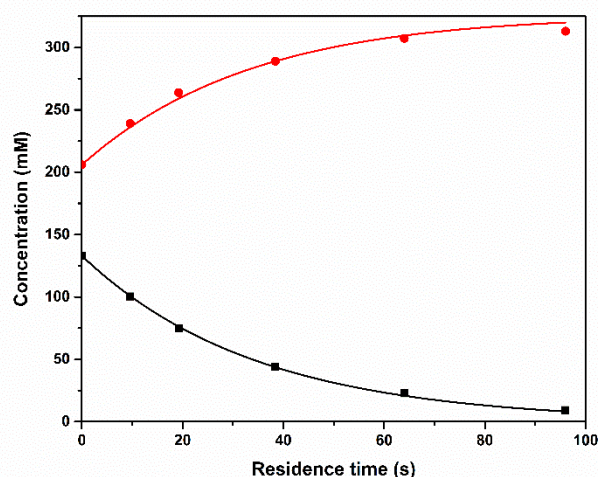


Figure 13. Xylose dehydration in presence of furfural with 5 mM HCl and at 498 K. Experiments were conducted with 2 wt% xylose and 2 wt% Furfural in a solvent system containing 80 wt% GVL. (a) Xylose and furfural concentration as a function of residence time. (b) Xylose conversion and furfural yield as a function of residence time. Black squares represent xylose and red circles represent furfural.

hydrogen ion concentration in aqueous media using mineral acids as catalysts. The reaction rates for both xylose and furfural disappearance were verified to be linear with respect to the acid concentration. Under these conditions, the rate equation for xylose consumption and furfural production can be written as:

$$\frac{d[\text{Xylose}]}{dt} = -k_1[\text{Xylose}][\text{H}_3\text{O}^+] - k_2[\text{Xylose}][\text{H}_3\text{O}^+] \quad [\text{Eq. (2)}]$$

$$\frac{d[\text{Furfural}]}{dt} = k_1[\text{Xylose}][\text{H}_3\text{O}^+] - k_3[\text{Furfural}][\text{H}_3\text{O}^+] \quad [\text{Eq. (3)}]$$

For the following initial conditions

$$@t = 0, [\text{xylose}] = [\text{xylose}]_0 \text{ and } [\text{Furfural}] = 0,$$

FULL PAPER

the rate equations can be solved to yield the following expression for the xylose and furfural concentrations as a function of the residence time.

$$[xylose] = [xylose]_0 \exp(-(k_1 + k_2)[H_3O^+]t) \\ = [xylose]_0 \exp(-(1 + \beta)[H_3O^+]k_1 t) \quad [\text{Eq. (4)}]$$

$$[Furfural] = [xylose]_0 \frac{k_1 \exp(-[H_3O^+]k_3 t)(1 - \exp(-[H_3O^+](k_1 + k_2 - k_3)t))}{k_1 + k_2 - k_3} \\ = [xylose]_0 \frac{\exp(-[H_3O^+]k_1 t)(1 - \exp(-[H_3O^+](1 + \beta - \alpha)k_1 t))}{1 + \beta - \alpha} \quad [\text{Eq. (5)}]$$

where, $\alpha = k_3/k_1$, $\beta = k_2/k_1$, and $k_i = k_i^{ref} \exp\left[-\frac{E_{a,i}}{R}\left(\frac{1}{T} - \frac{1}{T^{ref}}\right)\right]$.

k_i^{ref} is the rate constant for the i^{th} reaction measured at the reference temperature T^{ref} of 498 K, $E_{a,i}$ is the activation energy for the i^{th} reaction, T is the reaction temperature and R is the gas constant. The measured concentrations of xylose and furfural in Equation [Eq. (4)] and Equation [Eq. (5)] were fitted to the experimental data obtained at 473, 498 and 523 K to obtain the rate constants at 498 K and the activation energies of the individual reactions in Scheme 1. The values of the reaction kinetics parameters are reported in Table 1. Figure 14 shows the parity plot of xylose and furfural concentrations for the kinetic model described in Scheme 1. It can be seen from Figure 14 that the kinetic parameters reported in Table 1 are able to capture the reaction trends for various reaction condition studied. It is observed from Table 1 that the activation energies obtained in this work are lower than previously reported values.^[19,40,45] This result can be due to the stabilization of acidic protons by the polar aprotic solvent (GVL) leading to a decrease in the activation energy for acid catalyzed reactions, as described previously.^[35]

Table 1. Model-predicted reaction kinetics parameters (with associated 95 % confidence intervals) for xylose dehydration in GVL/H₂O solvent system.

	Rate constant at reference temperature $T^{ref} = 498K [L mol^{-1}s^{-1}]$		Activation energy $[kJ mol^{-1}]$
k_1^{498}	5.365±0.041	$E_{a,1}$	74.7±2.9
k_2^{498}	0.765±0.033	$E_{a,2}$	118.6±11.8
k_3^{498}	0.0285±0.0049	$E_{a,3}$	76.0±8.4

The activation energy for xylose degradation is higher than that of xylose dehydration (see Table 1), and it is predicted that higher temperature leads to lower furfural selectivity. A comparison of reaction time, reaction temperature and furfural yield is shown in Figure 15. It is observed from Figure 15 that higher temperature leads to lower furfural yield; however, as discussed above, the

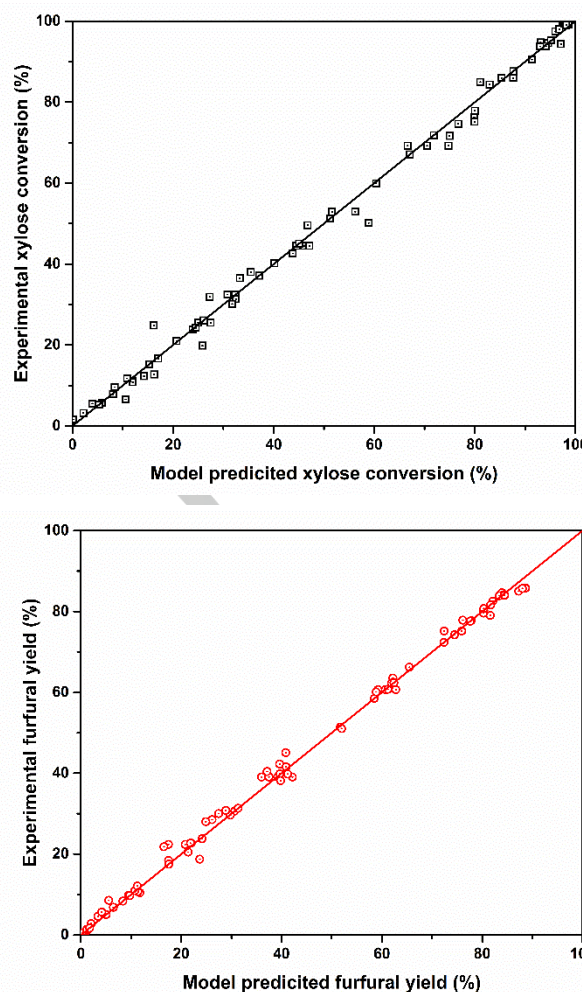


Figure 14. Parity plot of (a) xylose conversion and (b) furfural yield. Model predictions are from Scheme 1.

reaction temperature must be sufficiently high to suppress condensation reactions. We estimate from the kinetic model that high furfural yields (e.g., 90%) can be obtained for xylose dehydration conducted in the GVL/H₂O solvent system consisting of 80 wt% GVL and 10 mM hydrochloric acid at reaction temperatures between 480 and 500 K and at residence times near 100 sec. We note that there exists an optimal temperature range which suppress furfural loss due to condensation reactions leading to high furfural yield.

Production of furfural from lignocellulosic biomass:

The optimal conditions identified using the kinetic model were used for the production of furfural from maple wood. We used the solvent system composed of 80 wt% GVL and 20 wt% water containing 100 mM H₂SO₄ to depolymerize the hemi-cellulose

FULL PAPER

and the lignin fraction of biomass, while retaining the cellulose

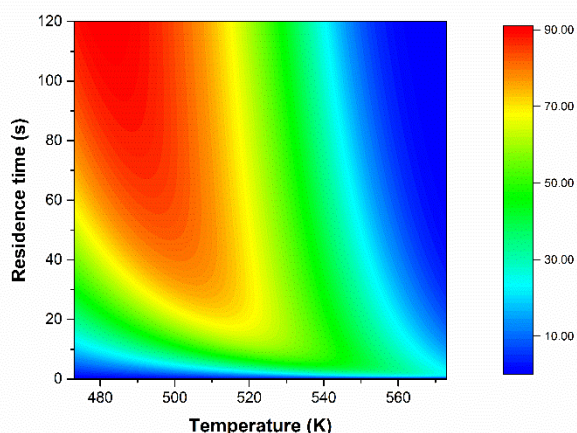


Figure 15. Model-predicted furfural yield as a function of residence time and reaction temperature. Acid concentration was fixed at 10 mM HCl.

fraction as a solid. For fractionation of maple wood, we used a 2-liter stirred Parr reactor fitted with a custom high-solids mixing system (described in Klingenberg et al.^[46] and Lutherbacher et al.^[47]) which led to effective mixing of biomass at high solid loading (10 wt% biomass). After 30 min at 403 K with a stirring rate of 60 rpm, 74% of the xylan present in the wood was recovered as soluble sugars in the hydrolysate (see Table 2). The soluble sugars were separated from unreacted cellulose by filtration, and the sugar solution was subjected to dehydration at 498 K for a residence time of 135 seconds. Under these reaction conditions, a furfural yield of 93% was achieved at 97% xylan conversion (see Table 2) and the kinetic model predicts complete xylose conversion and 85% furfural yield. The increased furfural yield obtained with the hydrolysate is due to the presence of xylose oligomers in the hydrolysate which are first hydrolyzed to xylose in the presence of acid, and the xylose thus produced is dehydrated to furfural leading to increased furfural yield. Also, it should be noted that no additional sulfuric acid was added to the hydrolysate before the dehydration reaction. Thus, our studies have identified processing conditions for production of furfural at high yields using high concentration of lignocellulosic biomass.

Table 2. Composition of maple wood, sugar concentration and yield after fractionation and after dehydration.

Composition of maple wood [wt%]			
Xylan	Glucan	Klason lignin	Moisture
19.3	41.9	24.9	5
Hydrolysate after fractionation			
Volume [ml]	C ₅ sugar conc. [wt%]	C ₅ sugar yield [%]	Furfural yield [%]
660	1.94	74.3	13.9
Hydrolysate after dehydration			
C ₅ sugars [wt%]	C ₅ sugar conversion [%]	Furfural yield [%]	Furfural conc. [wt%]
0.046	96.9	93.2	1.21

Conclusion

A monophasic solvent system comprised of GVL (80 wt%) and water (20 wt%) is used to produce high yields of furfural (>90%) from xylose as well as from lignocellulosic biomass. It is identified that the reaction temperature has the greatest influence on furfural yield, whereas the acid type, acid concentration and initial xylose concentration have minimal effect on furfural yield at complete xylose conversion. A reaction kinetic model is developed for the dehydration of xylose which involves three reactions: xylose dehydration to furfural, catalytic degradation of furfural and catalytic degradation of xylose. Moreover, it is shown that above a certain temperature (e.g., 473 K) the bimolecular condensation of furfural and xylose can be neglected, and it is possible to obtain high furfural yield (>90%). Through the kinetic model we identify that the optimal temperature range is from 480 to 500 K for xylose dehydration to furfural in the GVL/H₂O solvent system. The optimal conditions determined through the kinetic model are used to produce furfural from lignocellulosic biomass and furfural yield of 93% is achieved.

Experimental Section

Materials and experimental methods

D-(+)-xylose (≥99%), γ -valerolactone (≥99%), hydrochloric acid, sulfuric acid were purchased from Sigma-Aldrich and were used without further purification. Furfural (99%) was purchased from Sigma-Aldrich. The furfural was purified by distillation before use to remove polymers produced by self-condensation during storage.^[14] Furfural purity after

FULL PAPER

distillation was determined to be >99%. Distilled furfural was stored under Argon at 277 K and redistilled after 3 days in storage.

A schematic representation of the reactor system used for studying dehydration of xylose to furfural is shown in Figure 16. The flow-through reactor was comprised of a 20 cm glass lined stainless steel tube (1.0 mm internal diameter) (Trajan Scientific) with corresponding stainless steel valves and fittings (Swagelok). The heated zone of the reactor was fitted between two aluminum blocks placed within an insulated furnace. The volume of the heated zone of the reactor was 0.16 cm³. A type-K thermocouple (Omega) was placed at the reactor wall and was used to monitor and control the reactor temperature using a 16A series controller (Love). The reactor was pressurized using Argon, and the pressure was maintained at 550 psi for reaction at 473 and 498 K, 600 psi for 523 K throughout the reaction using a back pressure regulator. A GVL/H₂O solvent system consisting of 80 wt% GVL and 20 wt% H₂O, and containing the desired amount of xylose and mineral acid, was introduced at a specific flow rate using an HPLC pump to achieve the desired residence time. For reaction with a high concentration of xylose (10 wt%), two HPLC pumps were used to introduce the organic phase, containing GVL, and the aqueous phase consisting of water, xylose and sulfuric acid into the reactor. This approach was required because the solvent system separates into two phases at high xylose concentration (10 wt%) at low temperature (e.g., 303 K), but it becomes monophasic at reaction temperatures (>473 K). Liquid hydrolysate at the reactor outlet was collected in a separator and was periodically drained and analyzed for xylose and furfural concentrations using HPLC analysis.

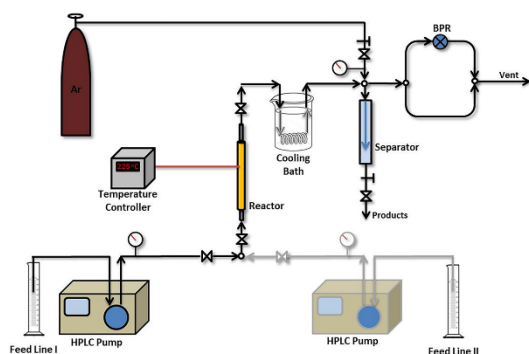


Figure 15. Model-predicted furfural yield as a function of residence time and reaction temperature. Acid concentration was fixed at 10 mM HCl.

Analysis

The concentrations of the reactant and products in the liquid hydrolysate were measured by High Performance Liquid Chromatography (HPLC) using a Bio-Rad Aminex HPX-87H column on a Waters 2695 system equipped with RI-2414 and PDA-2998 detectors. An aliquot of the product mixture was diluted 10 times with Milli-Q water (18 M Ω .cm) and filtered

with a 0.2 μ m PTFE filter before analysis. The temperature of the HPLC column was maintained at 338 K, and the flow rate of the mobile phase (pH=2 water, acidified by sulfuric acid) was kept constant at 0.6 ml/min. External calibrations with known standards were used to quantify reactant and product concentrations. Xylose concentration was measured with the RI detector, while furfural concentration was measured with the PDA detector (210 nm). Conversion of xylose and yield of furfural are calculated as follows.

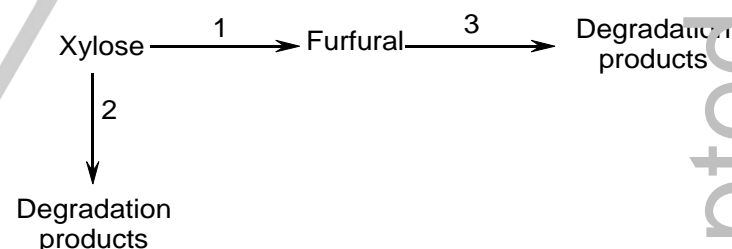
$$\text{Xylose conversion (\%)} = \frac{C_{xylose}^o - C_{xylose}}{C_{xylose}^o} \times 100$$

$$\text{Furfural yield (\%)} = \frac{C_{Furfural}}{C_{xylose}^o} \times 100$$

where C_{xylose}^o , C_{xylose} and $C_{Furfural}$ are the concentration of xylose in the feed, concentration of xylose in the product, and concentration of furfural in the product, respectively.

Reaction Kinetics Analysis

Experimental data were used to estimate the kinetic parameters of the proposed reaction kinetics models. For Scheme 1, the set of ordinary differential equation was solved to obtain an analytical solution. The kinetic parameters were estimated by minimizing the square of the sum of absolute errors between estimated and observed values at experimental sampling points using the non-linear optimization function in Matlab®. Additionally, separate experiments with only furfural as feedstock were performed to determine the kinetic parameters for furfural degradation (Scheme 1, reaction 3).



Scheme 1. Reaction network for xylose dehydration.

Acknowledgements

This material is based upon work supported by the DOE Great Lakes Bioenergy Research Center (DOE Office of Science BER DE-FC02-07ER64494).

Keywords: Furfural • γ -valerolactone (GVL) • Homogeneous catalysis • Sustainable Chemistry • Xylose

FULL PAPER

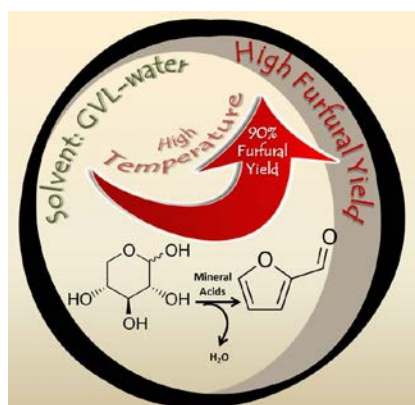
- [1] D. M. Alonso, S. G. Wettstein, M. A. Mellmer, E. I. Gurbuz, J. A. Dumesic, *Energy Environ. Sci.* **2013**, *6*, 76–80.
- [2] L. D. Schmidt, P. J. Dauenhauer, *Nature* **2007**, *447*, 914–915.
- [3] D. M. Alonso, J. Q. Bond, J. A. Dumesic, *Green Chem.* **2010**, *12*, 1493–1513.
- [4] M. J. Climent, A. Corma, S. Iborra, *Green Chem.* **2011**, *13*, 520–540.
- [5] Y. Gu, F. Jérôme, *Chem. Soc. Rev.* **2013**, *42*, 9550–9570.
- [6] L. Qi, I. T. Horváth, *ACS Catal.* **2012**, *2*, 2247–2249.
- [7] A. J. Ragauskas, C. K. Williams, B. H. Davison, G. Britovsek, J. Cairney, C. A. Eckert, W. J. Frederick, J. P. Hallett, D. J. Leak, C. L. Liotta, et al., *Science* **2006**, *311*, 484–489.
- [8] C. M. Cai, T. Zhang, R. Kumar, C. E. Wyman, *J. Chem. Technol. Biotechnol.* **2014**, *89*, 2–10.
- [9] R. Mariscal, P. Maireles-Torres, M. Ojeda, I. Sádaba, M. López Granados, *Energy Environ. Sci.* **2016**, *9*, 1144–1189.
- [10] R. H. Kottke, in *Kirk-Othmer Encycl. Chem. Technol.*, John Wiley & Sons, Inc., Hoboken, NJ, USA, **2000**, pp. 259–286.
- [11] G. W. Huber, J. N. Chheda, C. J. Barrett, J. A. Dumesic, *Science* **2005**, *308*, 1446–1450.
- [12] C. J. Barrett, J. N. Chheda, G. W. Huber, J. A. Dumesic, *Appl. Catal. B Environ.* **2006**, *66*, 111–118.
- [13] H. Schiweck, M. Munir, K. M. Rapp, B. Schneider, M. Vogel, in *Carbohydrates as Org. Raw Mater.* (Ed.: F.W. Lichtenthaler), Vch Weinheim, Germany, Berlin, **1991**, pp. 57–94.
- [14] K. J. J. Zeitsch, *The Chemistry and Technology of Furfural and Its Many By-Products*, Elsevier, **2001**.
- [15] C. Fang, W. Wu, H. Li, T. Yang, W. Zhao, Z. Wang, S. Yang, *Energy Sources, Part A Recover. Util. Environ. Eff.* **2017**, *39*, 2072–2077.
- [16] S. Zhang, J. Lu, M. Li, Q. Cai, *BioResources* **2017**, *12*, 2965–2981.
- [17] D. L. Williams, A. P. Dunlop, *Ind. Eng. Chem.* **1948**, *40*, 239–241.
- [18] I. C. Rose, N. Epstein, A. P. Watkinson, *Ind. Eng. Chem. Res.* **2000**, *39*, 843–845.
- [19] D. F. Root, J. F. Saeman, J. F. Harris, W. K. . Neill, *For. Prod. J.* **1959**, *9*, 158–165.
- [20] J. N. Chheda, Y. Román-Leshkov, J. A. Dumesic, *Green Chem.* **2007**, *9*, 342–350.
- [21] A. Mittal, S. K. Black, T. B. Vinzant, M. O'Brien, M. P. Tucker, D. K. Johnson, *ACS Sustain. Chem. Eng.* **2017**, *5*, 5694–5701.
- [22] C. Moreau, R. Durand, D. Peyron, J. Duhamet, P. Rivalier, *Ind. Crops Prod.* **1998**, *7*, 95–99.
- [23] A. S. Dias, M. Pillinger, A. A. Valente, *J. Catal.* **2005**, *229*, 414–423.
- [24] J. Zhang, J. Zhuang, L. Lin, S. Liu, Z. Zhang, *Biomass and Bioenergy* **2012**, *39*, 73–77.
- [25] E. I. Gürbüz, S. G. Wettstein, J. A. Dumesic, *ChemSusChem* **2012**, *5*, 383–387.
- [26] M. Yazdizadeh, M. R. J. Nasr, A. K. Safekordi, *Energy Sources, Part A Recover. Util. Environ. Eff.* **2018**, *40*, 125–133.
- [27] Q. Qing, Q. Guo, L. Zhou, Y. Wan, Y. Xu, H. Ji, X. Gao, Y. Zhang, *Bioresour. Technol.* **2017**, *226*, 247–254.
- [28] R. Xing, W. Qi, G. W. Huber, *Energy Environ. Sci.* **2011**, *4*, 2193–2205.
- [29] S. Peleteiro, V. Santos, J. C. Parajó, *Carbohydr. Polym.* **2016**, *153*, 421–428.
- [30] S. Peleteiro, S. Rivas, J. L. Alonso, V. Santos, J. C. Parajó, *Bioresour. Technol.* **2016**, *202*, 181–191.
- [31] I. Agirrezabal-Telleria, J. Reques, M. B. Güemez, P. L. Arias, *Green Chem.* **2012**, *14*, 3132–3140.
- [32] I. Agirrezabal-Telleria, C. Garcia-Sancho, P. Maireles-Torres, P. L. Arias, *Chinese J. Catal.* **2013**, *34*, 1402–1406.
- [33] L. Liu, H. Chang, H. Jameel, S. Park, *Bioresour. Technol.* **2018**, *252*, 165–171.
- [34] E. I. Gürbüz, J. M. R. Gallo, D. M. Alonso, S. G. Wettstein, W. Y. Lim, J. A. Dumesic, *Angew. Chemie Int. Ed.* **2013**, *52*, 1270–1274; *Angew. Chem.* **2013**, *125*, 1308–1312.
- [35] M. A. Mellmer, C. Sener, J. M. R. Gallo, J. S. Luterbacher, D. M. Alonso, J. A. Dumesic, *Angew. Chemie Int. Ed.* **2014**, *53*, 11872–11875; *Angew. Chem.* **2014**, *126*, 12066–12069.
- [36] H. Lin, J. Chen, Y. Zhao, S. Wang, *Energy & Fuels* **2017**, *31*, 3929–3934.
- [37] Y. Zhu, W. Li, Y. Lu, T. Zhang, H. Jameel, H. Chang, L. Ma, *RSC Adv.* **2017**, *7*, 29916–29924.
- [38] W. Li, Y. Zhu, Y. Lu, Q. Liu, S. Guan, H. Chang, H. Jameel, L. Ma, *Bioresour. Technol.* **2017**, *245*, 258–265.
- [39] D. M. Alonso, S. H. Hakim, S. Zhou, W. Won, O. Hosseinaei, J. Tao, V. Garcia-Negron, A. H. Motagamwala, M. A. Mellmer, K. Huang, et al., *Sci. Adv.* **2017**, *3*, e1603301.
- [40] R. Weingarten, J. Cho, W. C. Conner, Jr., G. W. Huber, *Green Chem.* **2010**, *12*, 1423–1429.
- [41] E. U. Franck, D. Hartmann, F. Hensel, *Discuss. Faraday Soc.* **1965**, *39*, 200–206.
- [42] W. L. Marshall, E. V. Jones, *J. Phys. Chem.* **1966**, *70*, 4028–4040.
- [43] G. Marcotullio, W. De Jong, *Green Chem.* **2010**, *12*, 1739–1746.
- [44] B. Vollmert, in *Polym. Chem.*, Springer Berlin Heidelberg, Berlin, Heidelberg, **1973**, pp. 33–321.
- [45] K. Lamminpää, J. Ahola, J. Tanskanen, *Ind. Eng. Chem. Res.* **2012**, *51*, 6297–6303.
- [46] D. J. Klingenberg, T. W. Root, S. Burlawar, C. T. Scott, K. J. Bourne, R. Gleisner, C. Houtman, V. Subramaniam, *Biomass and Bioenergy* **2017**, *99*, 69–78.
- [47] J. S. Luterbacher, A. Azarpira, A. H. Motagamwala, F. Lu, J. Ralph, J. A. Dumesic, *Energy Environ. Sci.* **2015**, *8*, 2657–2663.

FULL PAPER

FULL PAPER

Pushing the Limits on Furfural

Production: Furfural, a commodity chemical, is produced from the hemicellulose fraction of lignocellulosic biomass using a solvent system composed of γ -valerolactone and water. High temperature leads to efficient furfural production with minimal carbon loss. Optimal reaction conditions are identified to maximize furfural production from xylose as well as xylan.



Canan Sener, Ali Hussain
Motagamwala, David Martin Alonso,
and James A. Dumesic*

Page No. – Page No.

**Enhanced Furfural Yields from
Xylose Dehydration in the γ -
Valerolactone/Water Solvent System
at Elevated Temperatures**

Accepted Manuscript